

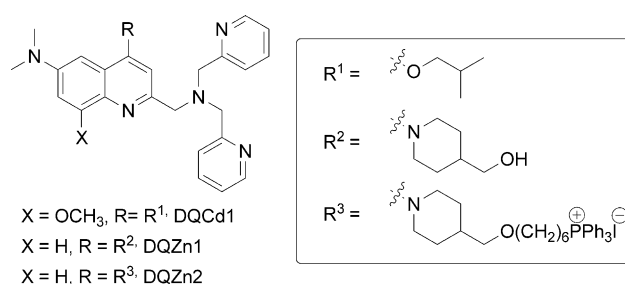
# A Ratiometric and Targetable Fluorescent Sensor for Quantification of Mitochondrial Zinc Ions

Lin Xue, Guoping Li, Cailan Yu, and Hua Jiang\*<sup>[a]</sup>

After several decades of development, fluorescent sensors have been recognised as indispensable and efficient molecular tools that can help monitor and visualise cations or biomolecules with high sensitivity and spatial resolution in live cells or tissues.<sup>[1]</sup> Undoubtedly, our understanding of metal ion homeostasis in biology has significantly benefited from advancements of fluorescent sensors for metal ions.  $Zn^{2+}$  has attracted significant attention because of its critical role in many biological processes.<sup>[2]</sup> In spite of worthy attentions on cytosolic  $Zn^{2+}$ , the function of  $Zn^{2+}$  in subcellular compartments, such as mitochondria, endoplasmic reticulum, and Golgi, and underlying dependence between these  $Zn^{2+}$  and cellular processes are still not established well.<sup>[3]</sup> Hence, developing targetable fluorescent sensors for monitoring the zinc level in specific organelles will contribute significantly to addressing these issues.

Since the fluorescent sensor TSO was first applied to in vitro imaging of  $Zn^{2+}$ ,<sup>[4]</sup> numerous  $Zn^{2+}$  sensors have been archived in the past few years. However, only a few small-molecule fluorescent or genetically encoded zinc sensors have been designed to target organelles.<sup>[3g,5]</sup> Moreover, most of these sensors read out the ion-binding event by emission intensity changes based on the photoinduced electron transfer (PeT) mechanism. Theoretically, this type of sensor can provide quantitative measurements of  $Zn^{2+}$ , but it is infeasible to quantify  $Zn^{2+}$  in live cells by these zinc fluorescent sensors because their emission intensity is significantly influenced by many other factors, such as the sample environment, sensor concentration, bleaching, and instrumental efficiency. A ratiometric sensor with self-calibration with dual emission maxima can eliminate most or all ambiguities and could be an ideal solution for quantitatively measuring intracellular ions.<sup>[6]</sup> So far, various ratiometric  $Zn^{2+}$ -selective sensors are available,<sup>[7]</sup> but unfortunately, only several examples of ratiometric and targetable sensors have been realised.<sup>[3g,5d]</sup> Design of targetable and ratiometric sensors for quantification of  $Zn^{2+}$  in specific organelles is, therefore, important, yet remains as one of the greatest challenges.

To this end, we designed a fluorescent sensor, DQZn2, for ratiometric detection of mitochondrial  $Zn^{2+}$  (Scheme 1). On



Scheme 1. Structures of DQCd1, DQZn1 and DQZn2.

the basis of our and other observations, 2-picolylamine (DPA) was employed as an ion chelator that was installed on the 2-position of quinoline platform so as to achieve high selectivity for  $Zn^{2+}$  over biological  $Na^+$ ,  $K^+$ ,  $Ca^{2+}$ , and  $Mg^{2+}$  with 1:1 stoichiometry and high affinity with nanomolar or lower  $K_d$  values.<sup>[8]</sup> In the meanwhile, to increase basicity of the sensor, the stronger electron donating nitrogen atom replaced the oxygen atom on 4-position of quinoline. We anticipated that this sensor could be protonated under neutral or even weakly basic media, and consequently would yield a resonance between quinolinium and onium resonant structures as observed for DQCd1.<sup>[9]</sup> The resonance would lead to charge delocalisation, which is more pronounced in the excited state of the molecule, due to occurrence of intramolecular charge transfer (ICT) in polar media.<sup>[10]</sup> We envisioned that  $Zn^{2+}$  coordination would induce the deprotonation of the sensor and consequent inhibition of the resonance. The ratiometric measurements with distinct emission maxima shift can thus be established. On the other hand, mitochondria are known to be one of sites that take up  $Zn^{2+}$  in living cells. It is implicated that the elevation of mitochondrial  $Zn^{2+}$  could lead to intracellular  $H_2O_2$  accumulation and mitochondrial dysfunction.<sup>[3c, 11]</sup> Therefore, it is important to quantify  $Zn^{2+}$  levels in mitochondria. The triphenylphosphonium salt (TPP), an effective mitochondrial targeting group, was thus chosen and attached to the sensor.<sup>[12]</sup> To minimise the influence of the TPP group on the photophysical properties of the sensor, it was separated from the fluorophore by long linkers.<sup>[5e]</sup> Furthermore, DQZn1, was also prepared as a control sensor. The synthesis procedures are described in the Supporting Information.

[a] L. Xue, G. Li, C. Yu, Prof. H. Jiang  
Beijing National Laboratory for Molecular Sciences  
CAS Key Laboratory of Photochemistry, Institute of Chemistry  
Chinese Academy of Science  
Beijing, 100190 (P.R. China)  
E-mail: hjjiang@iccas.ac.cn

Supporting information for this article is available on the WWW under <http://dx.doi.org/10.1002/chem.201103007>.

Both sensors had good solubilities ( $\sim 20 \mu\text{M}$ , Figure S1 in the Supporting Information) in aqueous buffer.

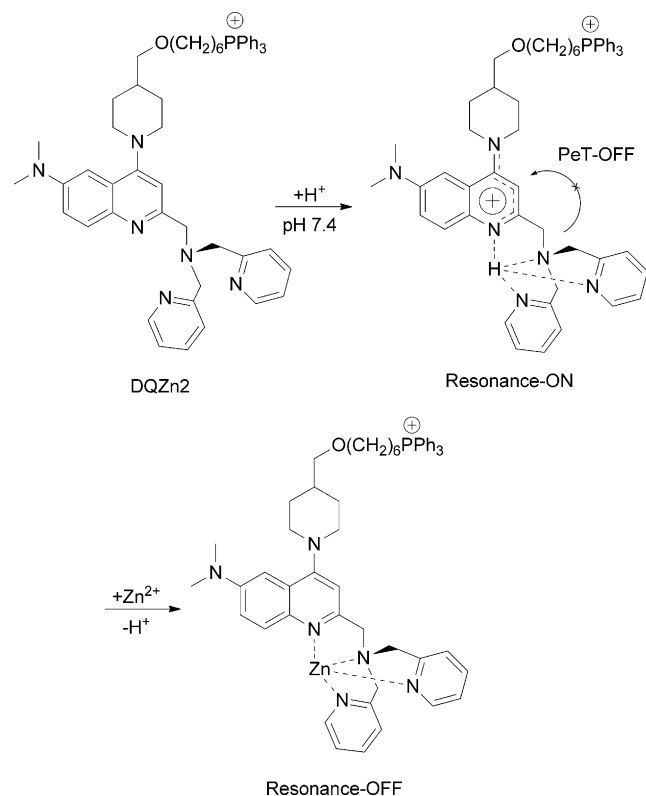
Firstly, by measuring pH dependence in aqueous buffer we found that DQZn1 has two  $\text{p}K_{\text{a}}$  values,  $\text{p}K_{\text{a}1}=8.05$  and  $\text{p}K_{\text{a}2}=4.84$  (Figure S2 in the Supporting Information). As expected, the  $\text{p}K_{\text{a}1}$  value of DQZn1 is obviously larger than that of DQCd1 (Table 1); this demonstrates that the basicity

Table 1. Spectroscopic properties of the sensors and their zinc complexes.<sup>[a]</sup>

Sensor	$\text{p}K_{\text{a}1}$	$\text{p}K_{\text{a}2}$	$\lambda_{\text{em}}$ [nm], <sup>[b]</sup> $\Phi$ <sup>[c]</sup>	ligand	complex
DQCd1 <sup>[d]</sup>	$7.31 \pm 0.01$	$4.46 \pm 0.02$	558, 0.17		510, 0.06
DQZn1	$8.05 \pm 0.02$	$4.84 \pm 0.01$	550, 0.11		507, 0.15
DQZn2	$7.66 \pm 0.02$	$4.57 \pm 0.02$	550, 0.11		504, 0.22

[a] HEPES (10 mM), NaCl (0.1 M), pH 7.4, 25 °C. [b] The maximum emission intensity. [c] Quinine sulfate was used as the standard for quantum yield measurements; [d] see ref. [9].

of DQZn1 is stronger and the nitrogen atom is a better donor than the oxygen atom to afford the resonance charge transfer. DQZn2 has similar protonation behaviour to DQCd1 and DQZn1 with two  $\text{p}K_{\text{a}}$  values of 7.66 and 4.57. The four nitrogen atoms including the DPA moiety and the quinolinic nitrogen form a proton binding pocket for the proton (Scheme 2);<sup>[13]</sup> this results in a combined  $\text{p}K_{\text{a}1}$  value and suppression of the photo-induced electron transfer (PeT) quenching from the tertiary amine of the DPA moiety. Therefore, DQZn2 displays considerable fluores-



Scheme 2. Proposed ratiometric sensing strategy.

cence emission ( $\lambda_{\text{em}}=550 \text{ nm}$ ,  $\Phi=0.11$ ) in aqueous buffer. Although a longer spacer (C6) was chosen to bridge the TPP and piperidino groups to minimise the effect of TPP on the properties of the fluorophore, the  $\text{p}K_{\text{a}1}$  value of DQZn2 was still about 0.4 units lower in comparison with that (8.05) of its precursor, DQZn1. This is presumably because of the repulsion effect from the positive charge on the TPP group, which is unfavourable for protonation and resonant charge delocalisation.

DQZn2 exhibited fluorescence maxima at 550 nm with quantum yield of 0.11 in HEPES buffer (10 mM HEPES, 0.1 M NaCl, pH 7.4). Upon addition of  $\text{Zn}^{2+}$  to the DQZn2 solution, the emission intensity at around 450–560 nm increased significantly, but the emission intensity at about 570–670 nm decreased slightly with an isoemissive point at 567 nm (Figure 1 and Figure S3 in the Supporting Informa-

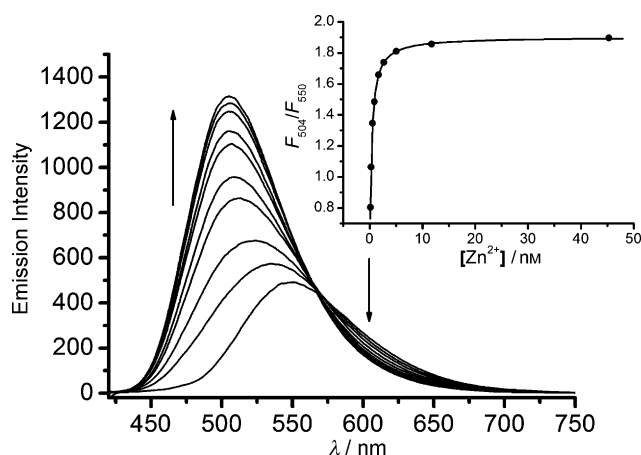


Figure 1. Fluorescence spectra of  $10 \mu\text{M}$  DQZn2 in the presence of free  $\text{Zn}^{2+}$  (0–45 nM). The free  $\text{Zn}^{2+}$  was regulated by using the NTA- $\text{Zn}^{2+}$  (0–1.8 mM) buffer (10 mM HEPES, 0.1 M NaCl, 2 mM NTA, pH 7.4,  $\lambda_{\text{ex}}=405 \text{ nm}$ ). Inset: the ratio changes ( $F_{504}/F_{550 \text{ nm}}$ ) as a function of  $\text{Zn}^{2+}$  concentration. The solid lines represent the nonlinear least-squares fits to the experimental data; NTA: nitrilotriacetic acid.

tion). The blue shift of 46 nm in the emission maxima (from 550 to 504 nm) and twofold enhancement in quantum yield demonstrates that  $\text{Zn}^{2+}$  kicked off the proton at the quinolinic site by coordination and subsequently inhibited resonance. The ratios of emission intensity ( $F_{504}/F_{550 \text{ nm}}$ ) were found to be 0.39 and 1.94 in the absence and presence of  $\text{Zn}^{2+}$ , respectively; this clearly indicates that DQZn2 is an excellent ratiometric fluorescent sensor for  $\text{Zn}^{2+}$  based on the mechanism of inhibition of resonance. The dissociation constants ( $K_{\text{d}}$ ) of DQZn2 were determined by using nonlinear least-squares fit analysis of the ratio of the emission intensity at selected wavelengths in  $\text{Zn}^{2+}$ -NTA buffered solutions (Figure 1 and Figure S5a in the Supporting Information). As expected, DQZn2 displayed a favourable  $K_{\text{d}}$  of  $0.45(\pm 0.01) \text{ nM}$ , and met the requirement for intracellular  $\text{Zn}^{2+}$  measurements. The Hill plots of the sensor confirmed the formation of a 1:1 DQZn2/ $\text{Zn}^{2+}$  complex (Figure S5b in the Supporting Information). Moreover, considering the fact

that mitochondria are more basic than the cytosol,<sup>[14]</sup> the fluorimetric titration experiments were repeated in more basic media (10 mM HEPES, 0.1 M NaCl, pH 8.0). As expected, the photophysical response of DQZn2 to Zn<sup>2+</sup> was not seriously disturbed (Figure S4 in the Supporting Information). The dissociation constant of DQZn2 was also measured in more basic solutions (pH 8) in the presence of NTA to be 0.15(±0.02) nM (Figure S5a in the Supporting Information). Thus, we believe that DQZn2 can respond to subnanomolar Zn<sup>2+</sup> and monitor the Zn<sup>2+</sup> level in mitochondria with sufficient sensitivity.

To study the selectivity of DQZn2 for Zn<sup>2+</sup>, its fluorescent properties in the presence of various cations were examined in aqueous buffer (Figure 2 and Figure S6 in the

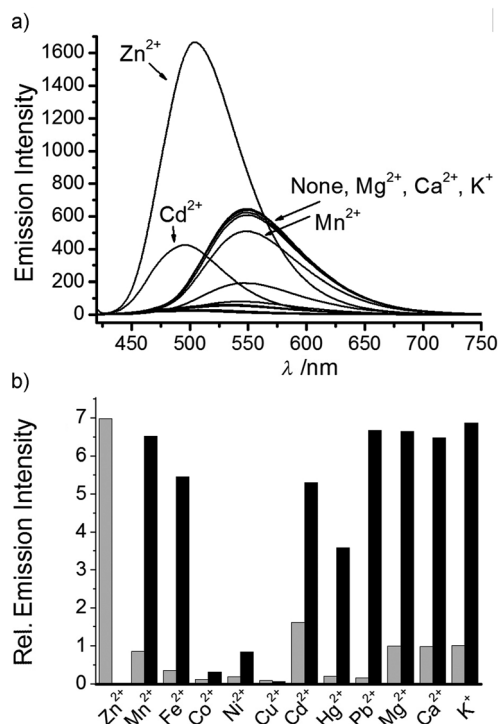


Figure 2. a) Fluorescence spectra of DQZn2 (10 μM) in the presence of various metal ions (10 μM Mn<sup>2+</sup>, Fe<sup>2+</sup>, Co<sup>2+</sup>, Ni<sup>2+</sup>, Cu<sup>2+</sup>, Zn<sup>2+</sup>, Cd<sup>2+</sup>, Hg<sup>2+</sup>, Pb<sup>2+</sup>, and 1 mM Mg<sup>2+</sup>, Ca<sup>2+</sup>, and K<sup>+</sup>) in buffer solution (10 mM HEPES, 0.1 M NaCl, pH 7.4, λ<sub>ex</sub> = 405 nm). b) Metal ion selectivity profiles of DQZn2 (10 μM). Gray bars represent the relative emission intensity (F/F<sub>0</sub>, at 504 nm) of DQZn2 in the presence of various metal ions. Black bars represent the fluorescence intensity of DQZn2 in the presence of the indicated metal ions, followed by Zn<sup>2+</sup> (10 μM).

Supporting Information). As expected, the biologically abundant metal ions, such as Na<sup>+</sup>, K<sup>+</sup>, Ca<sup>2+</sup>, and Mg<sup>2+</sup>, did not produce obvious effect on the fluorescence or ratio calibration of DQZn2 at millimolar concentration (1 mM), while Fe<sup>2+</sup>, Co<sup>2+</sup>, Ni<sup>2+</sup> and Cu<sup>2+</sup> strongly quenched the fluorescence as observed in many other sensory systems. These free cations would induce no obvious influence in vivo due to their extremely low concentrations. It should be noted that Cd<sup>2+</sup>, which exhibits many properties similar to those of Zn<sup>2+</sup>, did not enhance fluorescence (Figure 2a). Further-

more, the competition experiments indicate that Ca<sup>2+</sup>, Mg<sup>2+</sup>, and K<sup>+</sup> exerted negligible effect on Zn<sup>2+</sup> sensing by both intensity and ratio calibration.

Furthermore, we examined the pH-dependence of DQZn2 and its Zn<sup>2+</sup> complex (Zn–DQZn2) through the ratiometric responses (Figure S7 in the Supporting Information). In the biological pH range of 5–8, the ratio values of both DQZn2 and Zn–DQZn2 were almost insensitive. This indicates that pH changes do not affect the ratiometric signal output of DQZn2 under physiological conditions.

Before the cellular imaging experiments, we measured the cytotoxicity of DQZn2 using the CCK-8 assay. The results demonstrate that DQZn2 is almost nontoxic over a 24 h period (Table S1 in the Supporting Information) and the TPP targeting group did not obviously alter the cytotoxicity. To confirm whether DQZn2 is able to localise to mitochondria, a colocalisation experiment was performed by co-staining NIH3T3 cells with the commercially available markers LysoTracker Red DND-99 (Figure S8 in the Supporting Information), which is a lysosomal marker, and MitoTracker Deep Red (Figure 3b), which is a mitochondrial tracker.

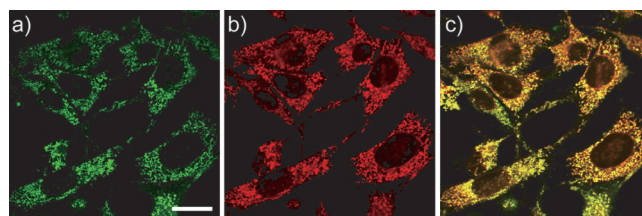


Figure 3. DQZn2 colocalises to mitochondria in live NIH3T3 cells. Cells were stained with: a) DQZn2 (1.5 μM), and b) MitoTracker Deep Red (50 nM) for 30 min at 25 °C in DMEM; c) overlay of a) and b); scale bar: 20 μm.

The fluorescence observed from DQZn2 and MitoTracker overlapped very well (Figure 3c) with a Pearson's colocalisation coefficient of 0.86, whereas the colocalisation coefficient between DQZn2 and LysoTracker was only 0.23; this indicates that DQZn2 is mainly localised to mitochondria in live cells.

Next, we employed DQZn2 to detect the mitochondrial Zn<sup>2+</sup> levels in living NIH3T3 cells. Incubation (30 min, in serum-free DMEM) of the cells and subsequent washing with phosphate buffered saline (PBS) afforded a stained sample that showed clear fluorescence at dual-emission channels of 430–490 nm (green) and 520–580 nm (red) under 405 nm excitation (Figure S9 in the Supporting Information). The ratio calculated as F<sub>green</sub>/F<sub>red</sub> gave an average value of 1.17 ± 0.045. Upon treatments with a low dose of ZnSO<sub>4</sub> (25 μM) and 2-mercaptopyridine *N*-oxide (10 μM) for 2 min, the ratio rapidly increased to 1.59 ± 0.093 (*P* < 0.001, *n* = 5). Sequestration of Zn<sup>2+</sup> with the membrane-permeable chelator TPEN (50 μM; *N,N,N',N'*-tetrakis(2-pyridylmethyl)ethylenediamine) rapidly reversed the ratio signals; this indicates that the increase in ratio depends on mitochondrial Zn<sup>2+</sup> changes (Figure 4). However, the membrane

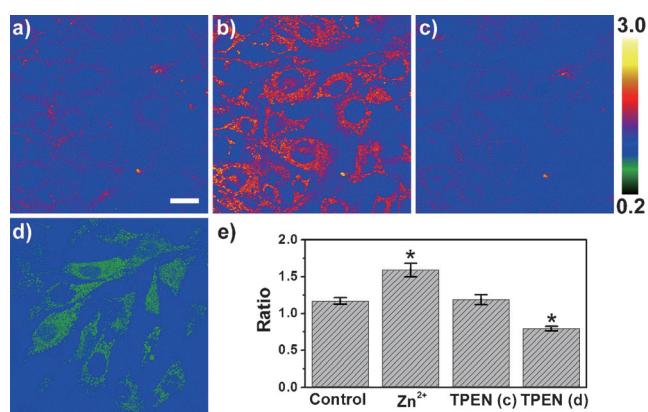


Figure 4. Fluorescence ratio images of DQZn2-labelled ( $1.5 \mu\text{M}$ ) NIH3T3 cells in PBS. a) Image of the emission window  $F_{\text{green}}/F_{\text{red}}$ ; scale bar:  $20 \mu\text{m}$ ; ratio bar: 0.2–3.0. b) Cells were treated with  $\text{ZnSO}_4$  ( $25 \mu\text{M}$ ) and 2-mercaptopyridine *N*-oxide ( $10 \mu\text{M}$ ) for 2 min. c) Cells were treated with TPEN ( $50 \mu\text{M}$ ) for 5 min. d) NIH3T3 cells were supplemented with TPEN ( $10 \mu\text{M}$ ) in the growth medium for 15 min and incubated with DQZn2 ( $1.5 \mu\text{M}$ ) for 30 min. e) Statistical analyses were performed with a two-tailed Student's *t*-test ( $n=5$ ) relative to the control. Asterisk (\*) indicates  $P < 0.01$ , and error bars are  $\pm$ SEM. The ratio ( $F_{\text{green}}/F_{\text{red}}$ ) was calculated as  $\text{Em}_{430-490}/\text{Em}_{520-580 \text{ nm}}$  upon 405 nm excitation.

potential sensitive dye, Rhodamine 123, did not show statistically significant changes with  $\text{ZnSO}_4$  and pyrithione treatment; this suggests that the ratio changes did not result from mitochondrial membrane potential changes (Figure S10 in the Supporting Information). Moreover, we pre-treated the cells with TPEN ( $10 \mu\text{M}$ ) in the growth medium for 15 min to suppress  $\text{Zn}^{2+}$  exchange in the mitochondria and then incubated them with DQZn2 for 30 min at  $25^\circ\text{C}$ . We found that TPEN leads to a significant decrease in the ratio ( $r = 0.79 \pm 0.033$ ) in contrast to the case without TPEN; this indicates that DQZn2 can be used to image  $\text{Zn}^{2+}$  fluctuations in mitochondria.

For quantitative analysis of this variable  $\text{Zn}^{2+}$  pool, the intracellular dissociation constant was calibrated according to a known procedure.<sup>[3e,15]</sup> The intracellular mitochondrial  $\text{Zn}^{2+}$  level was maintained by using HEPES buffer (20 mM HEPES, 0.1 M NaCl, 1 mM CaEDTA) with known concentrations of free  $\text{Zn}^{2+}$ . The mean ratio values for each well were plotted and an apparent  $K_d$  of  $77(\pm 18) \mu\text{M}$  was extracted from the calibration curve from the microscope by using nonlinear least-squares fit analysis (Figure S12 in the Supporting Information). The value is in accord with the fitted  $K_d$  of  $150(\pm 20) \mu\text{M}$  in pH 8.0 buffer solutions obtained by using the fluorometer. Therefore, this fluctuating mitochondrial  $\text{Zn}^{2+}$  concentration was calculated to be  $72(\pm 15) \mu\text{M}$  ( $n=5$ ) by using the corrected dissociation constant.

Since DQZn2 can monitor intracellular  $\text{Zn}^{2+}$  concentration changes with high sensitivity, we used this chemical tool to detect the mitochondrial homeostasis in endogenous zinc release. It is generally acknowledged that nitric oxide is an important regulator for both physiology and pathology. NO has been found to induce *S*-nitrosation and conformational changes of intracellular metallothionein (MT), and conse-

quent  $\text{Zn}^{2+}$  release from these MT to the cytoplasm.<sup>[16]</sup> Therefore, we made use of this molecule to elevate the cytosolic  $\text{Zn}^{2+}$  concentration in NIH3T3 cells. As shown in Figure 5 and Figure S11 in the Supporting Information, the

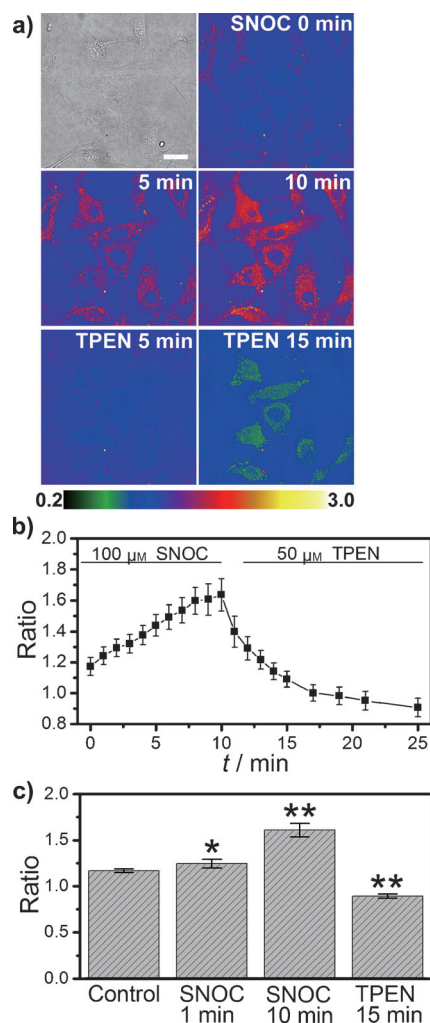


Figure 5. a) Fluorescence ratio images of DQZn2-labelled ( $1.5 \mu\text{M}$ ) NIH3T3 cells in PBS, treated with SNOC ( $100 \mu\text{M}$ ) and further treated with TPEN ( $50 \mu\text{M}$ ); scale bar:  $20 \mu\text{m}$ ; ratio bar: 0.2–3.0. b) Relative ratio value of emission intensity as a function of time. c) Statistical analyses were performed with a two-tailed Student's *t*-test ( $n=5$ ) relative to the control. Asterisk (\*) indicates  $P < 0.05$ , (\*\*) indicates  $P < 0.01$  and error bars are  $\pm$ SEM. The ratio ( $F_{\text{green}}/F_{\text{red}}$ ) was calculated as  $\text{Em}_{430-490}/\text{Em}_{520-580 \text{ nm}}$  upon 405 nm excitation.

dual-emission ratiometric imaging of the cells with DQZn2 showed that the ratio of  $F_{\text{green}}/F_{\text{red}}$  gradually increased after treatment with the NO donor *S*-nitrosocystein (SNOC,  $100 \mu\text{M}$ ),<sup>[17]</sup> and reached  $1.64 \pm 0.10$  ( $P < 0.01$ ,  $n=5$ ) after 10 min. The observed changes in the ratios were immediately decreased by TPEN treatment. These data demonstrate that the endogenously released  $\text{Zn}^{2+}$  was rapidly taken up by mitochondria within 1 min ( $P < 0.05$ ,  $n=5$ ), and establish that DQZn2 is able to monitor the mitochondrial  $\text{Zn}^{2+}$  level changes through the ratiometric approach. Thus, we believe

that DQZn2 is a prominent sensor for quantifying mitochondrial Zn<sup>2+</sup> levels in living cells and can be useful for investigations of mitochondrial Zn<sup>2+</sup> biology.

In summary, we present a quinoline-based ratiometric sensor, DQZn2, according to the principle of cation-induced inhibition of resonance. It allows single-excitation, dual-emission detection of Zn<sup>2+</sup> with significant blue shift of 46 nm in emission and remarkable changes in the ratio of fivefold in response to Zn<sup>2+</sup> with subnanomolar  $K_d$ , under physiological conditions. Moreover, we emphasise that DQZn2, which is attached with the TPP targeting group, can localised to the mitochondria in living cells and can indeed be used to visualise the changes of mitochondrial Zn<sup>2+</sup> level. Furthermore, we took advantage of DQZn2-stained ratiometric approach for quantification of the free mitochondrial Zn<sup>2+</sup> concentration in NIH3T3 cells. This molecular tool should be useful for investigations of mitochondrial Zn<sup>2+</sup> biology. The design strategy presented here is rational and practical for developing new ratiometric sensors for other biologically relevant analytes in subcellular locales; this is currently in progress.

### Acknowledgements

We thank the National Natural Science Foundation of China (Nos. 90813002, 21102148, 21125205), National Basic Research Program of China (No. 2011CB935800), the "100 Talent" program of the Chinese Academy of Sciences, and the State Key Laboratory of Fine Chemicals, Department of Chemical Engineering, Dalian University of Technology (KF1001) for financial supports.

**Keywords:** biosensors • fluorescent probes • mitochondria • quinoline • zinc ions

- [1] a) D. W. Domaille, E. L. Que, C. J. Chang, *Nat. Chem. Biol.* **2008**, *4*, 168–175; b) T. Terai, T. Nagano, *Curr. Opin. Chem. Biol.* **2008**, *12*, 515–521.
- [2] a) X. Xie, T. G. Smart, *Nature* **1991**, *349*, 521–524; b) J. M. Berg, Y. Shi, *Science* **1996**, *271*, 1081–1085.
- [3] a) R. D. Palmiter, S. D. Findley, *EMBO J.* **1995**, *14*, 639–649; b) S. C. Burdette, S. J. Lippard, *Proc. Natl. Acad. Sci. USA* **2003**, *100*, 3605–3610; c) S. L. Sensi, D. Ton-That, P. G. Sullivan, E. A. Jonas, K. R. Gee, L. K. Kaczmarek, J. H. Weiss, *Proc. Natl. Acad. Sci. USA* **2003**, *100*, 6157–6162; d) D. J. Eide, *Biochim. Biophys. Acta* **2006**, *1763*, 711–722; e) R. A. Bozym, R. B. Thompson, A. K. Stoddard, C. A. Fierke, *ACS Chem. Biol.* **2006**, *1*, 103–111; f) A. Krätzel, W. Maret, *J. Biol. Inorg. Chem.* **2006**, *11*, 1049–1062; g) P. J. Dittmer, J. G. Miranda, J. A. Gorski, A. E. Palmer, *J. Biol. Chem.* **2009**, *284*, 16289–16297.
- [4] C. J. Frederickson, E. J. Kasarskis, D. Ringo, R. E. Frederickson, *J. Neurosci. Methods* **1987**, *20*, 91–103.
- [5] a) S. L. Sensi, D. Ton-That, J. H. Weiss, A. Rothe, K. R. Gee, *Cell Calcium* **2003**, *34*, 281–284; b) E. Tomat, E. M. Nolan, J. Jaworski, S. J. Lippard, *J. Am. Chem. Soc.* **2008**, *130*, 15776–15777; c) J. L. Vinkenborg, T. J. Nicolson, E. A. Bellomo, M. S. Koay, G. A. Rutter, M. Merckx, *Nat. Methods* **2009**, *6*, 737–740; d) Y. Qin, P. J. Dittmer, J. G. Park, K. B. Jansen, A. E. Palmer, *Proc. Natl. Acad. Sci. USA* **2011**, *108*, 7351–7356; e) G. Masanta, C. S. Lim, H. J. Kim, J. H. Han, H. M. Kim, B. R. Cho, *J. Am. Chem. Soc.* **2011**, *133*, 5698–5700.
- [6] K. W. Dunn, S. Mayor, J. N. Myers, F. R. Maxfield, *FASEB J.* **1994**, *8*, 573–582.
- [7] Selected examples: a) P. Carol, S. Sreejith, A. Ajayaghosh, *Chem. Asian J.* **2007**, *2*, 338–348; b) J. L. Vinkenborg, M. S. Koay, M. Merckx, *Curr. Opin. Chem. Biol.* **2010**, *14*, 231–237; c) M. D. Pluth, E. Tomat, S. J. Lippard, *Annu Rev Biochem.* **2011**, *80*, 333–355.
- [8] a) L. Xue, H. H. Wang, X. J. Wang, H. Jiang, *Inorg. Chem.* **2008**, *47*, 4310–4318; b) L. Xue, C. Liu, H. Jiang, *Chem. Commun.* **2009**, 1061–1063; c) K. Hanaoka, K. Kikuchi, H. Kojima, Y. Urano, T. Nagano, *J. Am. Chem. Soc.* **2004**, *126*, 12470–12476; d) X. Y. Chen, J. Shi, Y. M. Li, F. L. Wang, X. Wu, Q. X. Guo, L. Liu, *Org. Lett.* **2009**, *11*, 4426–4429.
- [9] L. Xue, G. P. Li, Q. Liu, H. H. Wang, C. Liu, X. L. Ding, S. G. He, H. Jiang, *Inorg. Chem.* **2011**, *50*, 3680–3690.
- [10] a) Z. Dega-Szafran, A. Kania, B. Nowak-Wydra, M. Szafran, *J. Mol. Struct.* **1994**, *322*, 223–232; b) P. Chou, C. Wei, *J. Phys. Chem.* **1996**, *100*, 17059–17066; c) D. Panda, D. Ghosh, A. Datta, *J. Photochem. Photobiol. A* **2009**, *207*, 254–259.
- [11] a) S. L. Sensi, H. Z. Yin, S. G. Carriedo, S. S. Rao, J. H. Weiss, *Proc. Natl. Acad. Sci. USA* **1999**, *96*, 2414–2419; b) S. L. Sensi, H. Z. Yin, J. H. Weiss, *Eur. J. Neurosci.* **2000**, *12*, 3813–3818; c) S. L. Sensi, P. Paoletti, A. I. Bush, I. Sekler, *Nat. Rev. Neurosci.* **2009**, *10*, 780–791.
- [12] a) B. C. Dickinson, C. J. Chang, *J. Am. Chem. Soc.* **2008**, *130*, 9638–9639; b) M. F. Ross, T. A. Prime, I. Abakumova, A. M. James, C. M. Porteous, R. A. J. Smith, M. P. Murphy, *Biochem. J.* **2008**, *411*, 633–645; c) B. C. Dickinson, D. Srikun, C. J. Chang, *Curr. Opin. Chem. Biol.* **2010**, *14*, 50–56; d) S. C. Dodani, S. C. Leary, P. A. Cobine, D. R. Winge, C. J. Chang, *J. Am. Chem. Soc.* **2011**, *133*, 8606–8616.
- [13] a) B. A. Wong, S. Friedle, S. J. Lippard, *J. Am. Chem. Soc.* **2009**, *131*, 7142–7152; b) D. Buccella, J. A. Horowitz, S. J. Lippard, *J. Am. Chem. Soc.* **2011**, *133*, 4101–4114.
- [14] a) J. Llopis, J. M. McCaffery, A. Miyawaki, M. Farquhar, R. Y. Tsien, *Proc. Natl. Acad. Sci. USA* **1998**, *95*, 6803–6808; b) M. Nakano, H. Imamura, T. Nagai, H. Noji, *ACS Chem. Biol.* **2011**, *6*, 709–715.
- [15] a) C. Cheng, I. J. Reynolds, *J. Neurochem.* **2002**, *71*, 2401–2410; b) S. L. Sensi, D. Ton-That, J. H. Weiss, *Neurobiol. Dis.* **2002**, *10*, 100–108.
- [16] L. L. Pearce, R. E. Gandle, W. Han, K. Wasserloos, M. Stitt, A. J. Kanai, M. K. McLaughlin, B. R. Pitt, E. S. Levitan, *Proc. Natl. Acad. Sci. USA* **2000**, *97*, 477–482.
- [17] K. D. Kröncke, V. Kolb-Bachofen, *Methods Enzymol.* **1999**, *301*, 126–135.

Received: September 25, 2011  
Published online: December 21, 2011